Magnetic Nanocomposite Paste: An Ideal High- μ, k and Q Nanomaterial for Embedded Inductors in High Frequency Electronic Applications

T.D. Xiao[1], X.Q. Ma[1], H. Zhang[1], D.E. Reisner[1], P.M. Raj[2], L. Wan[2], and R. Tummala[2]

Inframat Corporation, 74 Batterson Park Road, Farmington, Connecticut 06032, USA
Package Research Center, 813 Ferst Drive NW Georgia Research Institute of Technology, Atlanta, GA 30332-0560, USA

ABSTRACT

Current inductors are the major impediment for miniaturization of electronics, due to the lack of magnetic materials with suitable high frequency properties. Future economically viable miniaturized high frequency electronic components require a low loss high frequency magnetic nanocomposite paste that is compatible with the low temperature powered circuit board ("PCB") process. Inframat Corporation is pioneering the development of magnetic nanocomposites for high frequency electronic applications [1-8]. This paper reports the work of a magnetic nanocomposite pastes, including silica coated cobalt-BCB and Ni ferrite-epoxy that were investigated as candidate materials. Nanocomposite thick film structures (125-225 microns) were screen printed onto organic substrates. Parallel plate capacitors and single coil coplanar inductors were fabricated on these films to characterize the electrical and magnetic properties of these materials at low and high frequencies. Electrical characterization showed that the Co/SiO_2 nanocomposite sample has a permeability and a matching permittivity of ~10 at GHz frequency range making it a good embedded inductor candidate. Both composites retain high permeability at 1-2 GHz.

1. INTRODUCTION

Electronic systems are trending toward multi-functionality and higher miniaturization at ever higher speeds and lower costs. Analog mixed-signal chips require several different supply voltages and advanced power management, requiring external power conversion circuitry. Most board-level switching power supplies consist of one or more integrated circuits (ICs) with a few external passive components. Integration of power supplies with the mixed-signal circuit would enable more coordinated power management, lower chip count, and less printed-circuit board (PCB) area, and possibly lower cost. Key to the successful implementation of distributed power architecture is the availability of light weight, low profile and high power density inductors.

Current inductive components in a semiconducting chip are the major impediment for miniaturization of electronics, due to conventional microsized magnetic materials can only be used at very low frequencies, *e.g.*, high permeability bulk ferrites can only be used at less than 1 MHz frequencies, and bulk Ni-ferrites, although can be used below 100 MHz, but its permeability is only ~12. Thus, current commercial efficient converters are still designed to be operated <2 MHz frequency.

Although there are commercial high frequency power circuitry components exist today, most of them still uses bulk high frequency, ferrites (nickel ferrite, nickel zinc ferrite, YIG ferrite). Most of these inductors are either donut shape, or E-shaped. These high frequency inductors in the power circuitry are very bulky, and occupy a large volume of the power component. Due to there is not a commercially available magnetic paste that can be used at >2 MHz frequencies with low loss and high inductance. Most commercial high frequency embedded inductors are still designed with empty coil, without a magnetic component. Although these embedded inductors have very low loss, they are operated at the expense of extremely low inductance values (typically ~0.1-0.2 micro-Henry). Current efficient power circuit board requires an inductance in the neighborhood of micro-Henry inductance.

High frequency magnetic pastes have been commercially available since the early 1990's [9-16]. These pastes are formed by milling magnetic powders and then loading the magnetic material into a liquid binder. For high frequency applications, the magnetic material of choice is ferrite. Two types of binders have been used in the paste formulation; organics and polymers. Organic based ferrite pastes are used in the fabrication of chip inductors for low power analog and communications applications. The magnetic material provides increased inductance for a given inductor volume. This generally occurs at the expense of high loss. However in applications where volume is severely restricted, chip inductors provide an acceptable solution. Because of their small size (*e.g.*, 100 mils x 100mils) these devices are not suitable for power applications due to excessive device power dissipation.

During fabrication of a chip inductor the ferrite is screen printed on to a ceramic substrate and sintered at temperatures between 700°C to 900°C. Organics are burned off and the ferrite develops its magnetic properties

The resultant magnetic thick film is covered with a layer forming a portion of the inductor. This process is repeated as necessary to achieve the required inductance. The high sintering temperatures preclude this material from being used with the PCB technology which is the substrate technology used in virtually all power converter products regardless of the technology used. As this is a thin film technology, the resultant magnetic layers are less than a mil thick. High-frequency power converters require magnetic layer at least 4 mils thick.

Ferrite loaded polymers are also available. These materials are generally used to fabricate microwave absorbers. Their high dielectric and magnetic loss tangents precluded them from being used in circulator applications. However, the polymer binder is compatible with the low temperature processing of PCB processes. Results have been reported on developing ferrite polymer pastes. To date these pastes have not demonstrated the performance necessary for power converter applications. Permeability is very low, typically <3, compared to the permeability of >3 required for high frequency point of use power converter applications. Many manufacturers have also attempted to develop a ferrite/polymer paste for its point of use switching power supply technology and could only duplicate previously published results. As a result of their researches, they are convinced that the only possible solution to a low cost, low cure temperature magnetic paste would be based on magnetic nanocomposites.

Chakrabarti, et al [17], had prepared ferromagnetic thick films using a paste method for microwave applications. In their work, micrometer sized Mn-Ni-ferrite, Li-ferrite, and Mg-Mn-ferrite were ball milled with ethyl cellulose in isobutyl alcohol and glass powders for 40 h to form a paste, which was then screen printed on an Al_2O_3 substrate to form a 200 μm film. The film was sintered at ~800^{o}C to eliminate porosity. Although this technique produced a thick film with acceptable performance, it did not produce a high quality ferromagnetic film, because this coating contained a large amount of glass content, not conducive to magnetic properties. Another shortcoming is that this process required a high temperature sintering procedure. There are other similar works on preparing magnetic thick films using the paste method that consist of only microsized ferrites, *e.g.,* Mn-Zn-ferrite and Ni-Zn ferrite [18-20].

A revolutionary technological advancement is required to propel the leap-ahead cost, weight, reliability, and performance improvements demanded of future high frequency inductors. Nanocomposite thin films (<1 μm) with significantly improved high frequency properties have been developed based on the exchange coupling mechanism [21-23]. However, the thin film techniques cannot be used to produce the thick film (25 -100 μm) with required inductance. A magnetic nanocomposite paste technology, suitable for low temperature semiconductor processes that Inframat is developing will satisfy this PCB process.

Reducing the particle size and the separation between neighboring particles down to the nanoscale leads to *novel magnetic coupling phenomena* resulting in higher permeability and lower magnetic anisotropy. Magnetic nanocomposites show permeability value much higher than that obtainable from the conventional material due to the reduced eddy current losses and interparticle exchange coupling effects at very high frequencies. The exchange interaction, which leads to magnetic ordering within a grain, extends out to neighboring environments. The exchange interaction in nanocomposites also leads to a cancellation of magnetic anisotropy of individual particles and the demagnetizing effect, leading to ultrasuperior soft magnetic properties. By choosing a system with high tunneling excitation energy, a huge increase in the resistivity can be achieved through the nanocompositing technique.

Future economically viable miniaturized high frequency electronic components require a low loss high frequency magnetic nanocomposite pate that is compatible with the low temperature PCB process. By using a new magnetic nanocomposite it is possible to reduce the embedded inductor in size and increase its inductance.

2. SYNTHESIS AND FABRICATION

***Silica-coated Co Synthesis*:** Inframat's technology for the synthesis and processing of magnetic nanocomposite is different from the conventional metallic and ferrite materials. The Co/SiO_2 nanocomposie was synthesized using an aqueous solution reaction technique, which is capable of synthesizing a variety of nanomaterials including metal, oxides, and composites in large quantities. In the synthesis of Co/SiO_2 magnetic nanocomposite powders, experimental procedures include preparing the starting precursors containing Co and SiO_2, co-atomization of the precursors to form colloidal solution of Co and SiO_2 and annealing the colloidal solution to form Co/SiO_2 nanocomposite powders.

A typical TEM bright field image for Inframat's synthetic Co/SiO_2 nanocomposite is shown in Fig. 1. The TEM studies revealed that the synthetic nanocomposite is a two-phase material, where nanoparticles of Co are coated with a thin film of silica. The Co phase has an average particle size of ~30 nm. Selected area electron diffraction experiments indicated that the Co particles are FCC nanocrystals, where the matrix silica phase is amorphous [1-2].

In order to study the microstructure in detail at the nanometer level, localized regions at the Co/silica interface have been studied using a microbeam diffraction

technique. The diffraction beam was reduced to approximately 10 nm in size and diffracted at the area of interest. Two phases were found in localized regions, including FCC Co and γ-phase SiO_2. Majority SiO_2 coating is amorphous, as indicated in the XRD and other selected large area diffraction techniques [2].

The Co-Silica nanoparticles (50 wt.% each) were mixed with Benzo Cyclo Butene (BCB) polymer (Dow Chemicals, Midland, Michigan) using conventional mixing. The as-received BCB 3022-46 has 46 % volatile mesitylene. A paste (60 wt. % inorganic and 40 wt. % as received polymer) with suitable viscosity was then screen printed to a thickness of 225 microns onto high-temperature copper-clad FR-4 substrates that are compatible with BCB curing at 250 C. Copper is sputtered to a thickness of 3 microns, and patterned by an etch-back process to form the top electrode.

Ferrite synthesis: In the ferrite nanoparticles synthesis, again, a low temperature synthesis approach based on the aqueous synthesis method has been developed to synthesis very fine $(Ni_{0.5}Zn_{0.5})Fe_2O_4$ nanoparticles. The procedures include (1) preparation of a salt solution that contains Ni, Zn, and Fe with the selected atomic ratio, (2) addition of the NH_4OH solution into the Ni and Fe precursor solution to adjust pH, without any precipitation, (3) conversion of the precursor solution into a Ni-Fe-O complex powder, and (4), conversion of the Ni-Zn-Fe-O material into nano-$(Ni_{0.5}Zn_{0.5})Fe_2O_4$ at low temperature in oxygen controlled atmosphere.

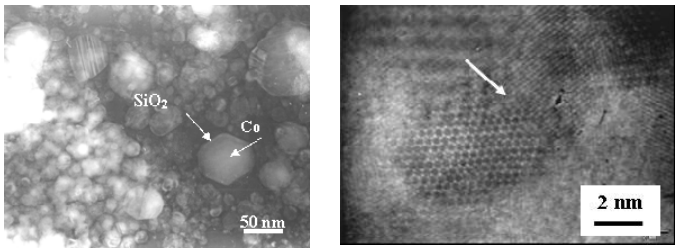

Fig 1. TEM micrograph shows a two phase material, where amophous SiO_2 films are coated on Co nanocrystal surfaces (left). A typical atomic resolution TEM micrograph showing the microstructure of the $(NiZn)Fe_2O_4$ nanoparticles (right). Arrow points to the boundary between two nanoparticles.

In the microstructure studies, HRTEM specimens were prepared by dispersing the powders in methanol. Drops of this solution were then deposited on a carbon-grit and observed in the microscope. Bright field images, electron diffraction, and lattice images were carried out. A typical HRTEM atomic resolution image shown the morphologies of the ferrite nanoparticle materials is illustrated in Fig. 1. TEM studies at atomic resolution and electron diffraction reveal that the synthetic $(NiZn)Fe_2O_4$ nanoparticle is hexagonal. The size of the ferrite nanoparticle is ~ 5 to 15 nm.

The nanoparticles of ferrite were dispersed into a commercial epoxy to form a thick paste. The paste is then screen-printed onto a FR4 substrate to a thickness of 125 microns. The composition of the paste consists of 50-70% nanoparticles uniformly dispersed in an epoxy resin. The epoxy can be cured to form a dense solid at temperatures between 80-120^{o}C. The curing time correspondingly varies from 5 h to 30 minutes. In this study, the films were cured at 120 ^{o}C for 30 minutes. The top electrode was sputtered to a thickness of 3 microns and patterned by an etch-back process.

3. ELECTRICAL CHARACTERIZATION

To perform low frequency initial permeability measurements, the as-formed pastes were poured into a mold. The cast pastes were then cured at 80^{o}C for 8 h to allow for hardening to form donut-type toroids. A typical photograph of cured Ni-Zn ferrite ($Ni_{0.5}Zn_{0.5}Fe_2O_4$) toid is shown in Fig. 2. The formed toroids were then winded with magnetic wires for permeability measurement using an Agilent 4192A impedance analyzer, with operation frequencies varies from 10 kHz to 13 MHz. The derived permeability is then plotted as a function of frequency as shown in Fig. 3 for a typical permeability v.s. frequency plot for a 46vol% Ni-Zn-ferrite with 54vol% epoxy nanocomposite paste.

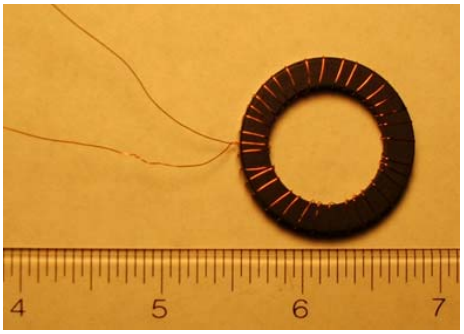

Fig. 2. A typical photo shown the cast and cured toroids for low frequency permeability measurement, the toroid dimension is 31.5mm (OD) × 21.4 (ID) × 4.7mm (thick), and with 34 turns of copper windings.

In general, at the frequency measured, the permeability has a very flat response as a function of frequencies. The permeability varies from 5 to 15 depending on the volume of ferrite loading in the epoxy, the tangent losses were less than 0.001 dB, and quality factors, (Q) in excess of 100, Q is for all the samples examined. With proper engineering, we expect a permeability of 20 can be achieved in the future, while retain its low loss aspects.

Parallel plate capacitor and single coil inductor structures were also fabricated to characterize the electrical properties of these materials. The structure details are

described in Fig. 4. Different sized components were used to check the consistency in the measurements and also for internal calibration.

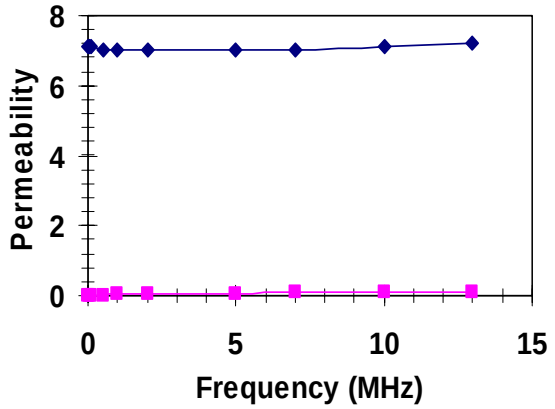

Fig. 3. Permeability as a function of frequency plot, from 10 KHz to 13 MHz, showing flat frequency response at measured frequencies, with low loss tangent, <0.001 dB, and high quality factor, Q>100.

Fig. 4. Fabricated inductor and capacitor structures. The outer diameter for the inductor coil is 1.22 mm while the inner diameter is 0.53 mm. The size of the capacitor is 2.33x 2.33 mm. For the capacitor, the adjacent metal is connected to the bottom electrode.

To characterize the permittivity, both high frequency and low frequency characterization techniques were employed. Low frequency characteristics were measured with a Precision LCR meter (Agilent 4285A). The dielectric constants of both the nanocomposites are much higher than the base polymer employed. The observed decrease in dielectric constant with frequency (Fig. 5) in metal-insulator composites is indicative of the interfacial polarization relaxation.

The high frequency measurements were conducted with an s-parameter Network Analyzer (HP Model 8720 ES). Two-port measurements were employed to eliminate any systematic errors that occur with single port measurements. The probes were ground-signal type with a spacing of 500 microns. Ground-Signal-Ground probes were not used in this study. The transfer impedance (Z_{12} or Z_{21}) can be estimated from the s-parameters as:

$$Z = 50\frac{2S_{12}}{(1-S_{11})(1-S_{22})-S_{12}S_{21}} \qquad (1)$$

for 2-port measurement with two probes located on the same position of a coupon. Another form of this relationship is also reported in the literature [24].

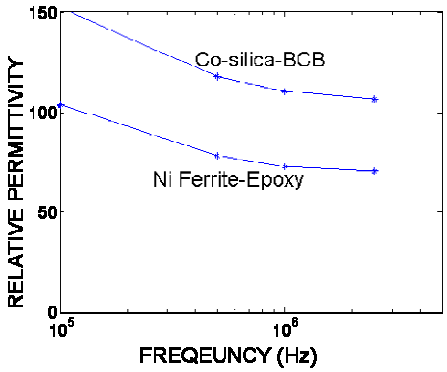

Fig. 5. Low frequency permittivity measurements of magnetic nanocomposites.

Equations for parallel plate capacitor: Different size of capacitors built on the same substrate, using same material and processing can be used for internal calibration. Below the first self-resonant frequency, a capacitor can be deemed equivalent to a capacitor, inductor and resistor connected in series. The equation for the serial circuit is expressed as:

$$Z = j\omega L + \frac{1}{j\omega C} + R \qquad (2)$$

where Z is the impedance of the equivalent circuit. L, C, and R are inductance, capacitance and resistance of the circuit respectively. ω is the angular frequency. L, C, and R are functions of frequency. Since there are three unknowns in the equation different size capacitors would be needed. The goal of this work is to extract permeability and permittivity. The equations for the two capacitors will be:

$$\mathrm{Im}(Z_1) = j\omega L_1 + \frac{1}{j\omega C_1} \qquad (3)$$

$$\mathrm{Im}(Z_2) = j\omega L_2 + \frac{1}{j\omega C_2} \qquad (4)$$

The geometric part of the capacitance, C_o, for parallel plate capacitor can be estimated using as $\varepsilon_0 \frac{A}{d}$ where A is the area of the plane and d is the distance of separation between the planes. There is no simple equation for the inductance. Generally, inductance with frequency dependent material can be expressed as: $L = \mu(f)L_0$ where L_0 is the inductance of an inductor filled with a non-magnetic material. The L_0 value can be estimated from the above equations by plugging in the permittivity and permeability measurements done independently at 50-100 MHz using bulk inductors at Inframat [1-2]. Using the estimated L_0 and C_0, the permeability and permittivity at all the other frequencies can be solved from the

simultaneous equations (3-4) for two capacitors. Figs. 6 and 7 show the permittivity and permeability values for both the nanocomposite systems. It is interesting to note that both materials retain a permittivity of more than 10 at GHz frequency. The permeability value for Co-Silica-BCB is close to 10 at 1 GHz frequency as seen in Fig. 7.

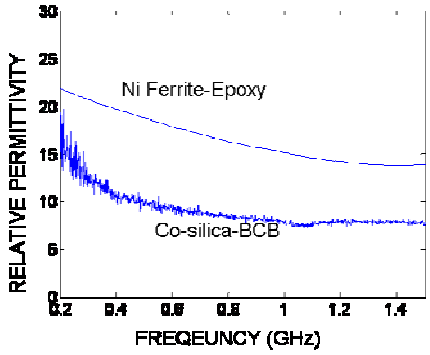

Fig. 6. High frequency permittivity of magnetic nanocomposites.

Estimation of permeability from inductor structures: Different size inductors were built on the magnetic nanocomposite substrate as well as a glass microslide with known permability of 1 and same thickness as the magnetic nanocomposite (125 microns). For the nanocomposite sample, the inductor is completely buried by screen printing the paste above and below the structure, while opening the pads for testing. Using same inductor structures on glass and nanocomposite, the permeability was directly estimated from the impedance measurements as:

$$\mu = \frac{\mathrm{Im}(Z)_{Nanocomposite}}{\mathrm{Im}(Z)_{Glass}} \qquad (5)$$

It should be noted that the actual equivalent circuit of the test structure is much more complicated, with an inductor and resistor in series, and a capacitor in parallel. The resistive effects, amplified by the loss, and capacitive effects, amplified by the high permittivity nanocomposite, significantly affect this estimate. Hence, this analysis is not suitable for higher frequencies, where the Im(Z) v.s. frequency deviates from a straight line. The obtained inductance v.s. frequency is plotted in Fig. 7, along with that of Co-Silica-BCB for comparison. The measurement indicates that the nanocomposite retains a permeability of 2.5 at 1 GHz frequency.

High frequency characteristics of metal-based magnetic nanocomposites were previously reported by Miura et al [4]. In their work, iron powder resin showed a permeability decreasing from 3 to 2, as the frequency increases from 1 GHz to 5 GHz. Similarly, $Ba_2Ni_2Fe_{12}O_{22}$ showed a steep decrease in permeability from 4.5 at 200 MHz to 2 at 1 GHz, as studied by Shin and Oh [5]. While the permeabilities of $Fe_{72}Al_{11}O_{17}$ and $Fe_{55}Al_{18}O_7$ are not stable beyond 1 GHz, $Co_{59}Zr_{12}O_{30}$ showed stable properties of 70-80 beyond 1 GHz. These are presumably not organic compatible materials. Polymer based composites showed a steep decrease in permeability from 10 at 1GHz to 1 at 3 GHz, as reported by Yoshida et al [6]. The Co-Silica-Polymer system showed higher permeability and permittivity than the polymeric magnetic nanocomposite systems reported in the literature because of its nanoparticle size and silica coating. The high frequency stability of the Ni ferrite permeability is always of concern, as is also seen in this study. The nanocrystalline Ni ferrite is expected to yield higher permeabilities than their bulk counterparts. One reason this was not observed in these studies could be the use of lossy polymer such as epoxy which could alter the inductive behavior considerably. High performance BCB is currently being used as the nanocomposite matrix to gain further improvement in properties.

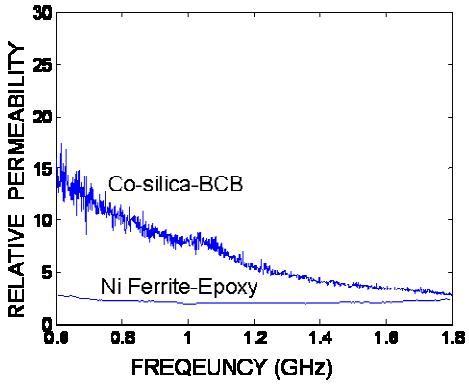

Fig. 7. High frequency permeability of magnetic nanocomposites.

The dielectric loss of Co-silica-BCB varied with the filler content. Incorporation of metal inside a polymer increases the dielectric loss. In the nanocomposites studied here, the silica coating is expected to prevent the charge leakage and help lower the losses. The low frequency dielectric loss of these nanocomposites varied from 0.003 for low filler content to 0.08 for higher filler content. Further improvements in the formulation and dispersion methodologies are now being investigated to lower the loss at high filler contents.

4. CONCLUSIONS

Thick films formed by ferrite-epoxy and Co-silica-BCB nanocomposite pastes were characterized for their permittivity and permeability over broad frequency range to assess their suitability for inductor and antenna applications. Interestingly, both materials show high permittivity and permeability. Co-silica-BCB shows matching permittivity and permeability of 5-10 making it a good candidate for miniaturized antennas. Fabricated inductor structures on Ni-Zn ferrite-epoxy showed that

the material retains a permeability of 5-15 at low MHz frequencies and 2.5-3 at GHz frequency range. Both material systems show significant advances over existing organic (Printed Wiring Board) compatible magnetic nanocomposites for high-frequency inductor applications.

5. ACKNOWLEDGMENTS

Dr. T. Danny Xiao and his co-workers thank Inframat Corp. for funding the research activities in conducting this work. Goergia's group is supported by the National Science Foundation (NSF) through the NSF ERC in Electronic Packaging (EEC-9402723) at Georgia Institute of Technology. The authors also than Venky Sundaram (PRC, Georgia Tech.) and Yong Kyu Yoon (ECE, Georgia Tech.) for their assistance.

6. REFERENCES

[1]. Y. D. Zhang, S. H. Wang, D. T. Xiao, J. I. Budnick and W. A. Hines, "Nanocomposite Co/SiO2 soft magnetic nanomaterials", *IEEE Trans. Magnetics*, **Vol. 37**, no. 4, July 2001, pp. 2275-2277.

[2]. Y.D. Zhang, S. Wang, and T.D. Xiao, "Insulator coated magnetic nanoparticulate composites with reduced core loss and method of mfg thereof," *US Patent No.* **6,720,074 B2** (April 13, 2004)

[3]. T.D. Xiao, *et al,* "Thick Magnetic Nanocomposite Films and Method Thereof," US Patent Appl. May, 2004.

[4]. T.D. Xiao, *et al,* "Tape Casting Nanostructured Components," US Patent filed June, 2004.

[5]. M.Z. Wu, Y. D. Zhang, S. Hui, **T. D. Xiao**, S. Ge, W. A. Hines, J. I. Budnick, and G. W. Taylor, "Microwave magnetic properties of $Co_{50}/(SiO_2)_{50}$ nanoparticles," *Appl. Phys. Lett.* **80**(23), 4404 (2002)

[6]. M.Z. Wu, S. Ge, J.I. Budnick, W.A. Hines, Y.D. Zhang, S. Hui, and **T.D. Xiao**,"Structure and Magnetic Properties of SiO_2-Coated Co Nanoparticles," *J. Appl. Phys.*, **92**, 491-494 (2002)

[7]. Z. Zhang, Y.D. Zhang, **T.D. Xiao**, S. Ge, M. Wu, W.A. Hines, J.I. Budnick, J.M. Gromek, M.J. Yacaman, and H.E. Troiani, "Nanostructured $NiFe_2O_4$ Soft Magnetic Ferrite," *Mat. Res. Soc.* **703**, pp. 111-116 (2002)

[8]. M. Wu, Y.D. Zhang, S. Hui, **T.D. Xiao**, S. Ge, W. A. Hines, J. I. Budnick, and M. J. Yacaman, "Magnetic properties of SiO_2-coated Fe nanoparticles," *J. Appl. Phys.* **92**(11), 6809 (2002)

[9]. Jin-Woo Park and Mark G. Allen, "Ultralow-profile micromachined power inductors with highly laminated Ni/Fe cores: Application to low-megahertz DC-DC converters", IEEE Transactions on magnetics, vol. 39, 5, Sept., 2003, pp. 3184-3186.

[10]. M. Xu, T. M. Liakopoulos, C. H. Ahn, S. H. Ahn and H. J. Kim, "A microfabricated transformer for high-frequency power or signal conversion", IEEE Trans. Magn., **vol. 34**, July, 1998, pp. 1369-1371.

[11]. C. R. Sullivan and S. R. Sanders, "Microfabrication process for high-frequency power-conversion transformers", in Proc. 26th Annual Power Electronics Specialists Conference, June 1995, pp. 658-664.

[12]. Y. Hisatsune, K. Sasaki, H. Ikegami, K. Okumura, "Semiconductor Device, its manufacturing process, position matching mark, pattern forming method and pattern forming device," *US Patent* **6,709,966** (2004)

[13]. J. Kato, O. Inoue, S. Nakatani, K. Hirano, and T. Asahi, "Magnetic element and method of manufacturing the same," *US Patent* **6,392,525** (May, 2002)

[14]. P.I. Mayo, I.T. Morgan, C.F. Norman, R.J.D. Nairne, "Surfce modification of magnetic particle pigments," *US Patent* **5,868,959** (February, 1999)

[15]. T. Yadav, C. Kostelecky, E. Franke, B. Miremadi, M. Au, and A. Vigliotti, "Nanomaterials and magnetic media with coated nanostructured fillers and carriers," *US Patent* **6,737,463** (May, 2004).

[16]. A. Hashimoto and Y. Takase, "Method of manufacturing ceramic thick-film printed circuit board," *US Patent* **6,753,033** (June, 2004)

[17]. N.B. Chakrabarti, C.K. Maiti, S. Kal, and D. Bhattaoharryya, "Microwave applications of Ferrimagnetic Pastes," Proc. Intn'l Symp. Hybrid Microelectronics (ISHM), pp 224-228, 1979, Los Angeles, USA

[18]. Y. Yamamoto, A. Makino, T. Yamaguchi, and I. Sosada, "Fine Grained Ferrite for Low Profile Transformer," *IEEE Transaction on Magnetics,* **33,** 3942-3944 (1997).

[19]. M.M. Riahi-Kashani and A. Elshabini-Riad, "Permeability of ferrite pastes, epoxies, and substrates over a wide range of frequencies," *IEEE Transaction on Instrumentation & Measurement,* **41,** 1036-1040 (1992).

[20]. M.M. Riahi-Kashani and A. Elshabini-Riad, "Characterization of Ferromagnetic Materials for Microelectronics applications over," *IEEE,* 430-435 (1992).

[21]. G. C. Hadjipanayis and G. A. Prinz, Science and Technology of Nanostructured Magnetic Materials, (plunum Press, New York, 1991)

[22]. Y. Hayakawa and A. Makino, H. Fujimori and A. Inoue, High resistive nanocrystalline Fe-M-O (M=Hf, Zr, rare-earth metals) soft magnetic films for high-frequency applications, *J. Appl. Phys.* **81**, 3747 (1997).

[23]. H. Fujimori, Structure and soft magnetic properties in multilayers and granular thin films, *Sripta Met. Mat*. **33** 1625 (1995).

[24] Istvan Novak, Jason R Miller, "Frequency – Dependent Characterization of Bulk and Ceramic Bypass Capacitors", Poster material for the *12th Topical Meeting on Electrical Performance of Electronic Packaging*, October 2003, Princeton, NJ.